

All-optical bistable switching in curved microfiber-coupled photonic crystal resonators

Myung-Ki Kim,^{a)} In-Kag Hwang,^{b)} Se-Heon Kim, Hyun-Joo Chang, and Yong-Hee Lee
Nanophotonics Laboratory, Department of Physics, Korea Advanced Institute of Science and Technology, Daejeon 305-701, Korea

(Received 1 February 2007; accepted 19 March 2007; published online 18 April 2007)

The authors report low-power optical bistability under continuous wave pumping conditions in five-cell photonic crystal linear resonators containing InGaAsP quantum wells, by employing the fiber-coupling technique. The threshold bistable power is measured to be $35 \mu\text{W}$ at the normalized detuning of -1.724 . Owing to the high band-edge nonlinearities of quantum wells and the efficient fiber coupling, minimal instability is observed. In addition, all-optical switching is demonstrated with switching energy less than 75.4 fJ . © 2007 American Institute of Physics.

[DOI: 10.1063/1.2724921]

One of the most interesting features of photonic crystal (PhC) resonator is the strong photon confinement in a small volume. This characteristic is of interest in quantum optics,¹ nonlinear optics,² lasers,³ and optical communications.⁴ For this reason, many groups have tried to realize high quality (Q) factor PhC resonators with small mode volumes. Among many applications using PhC resonators, we focus on low-power all-optical devices, such as optical memories, optical switches, and optical logic gates. Especially, the optical bistability is simple and robust paradigm for all-optical transistors and memories.⁵ In bistable devices, two stable output states are allowed for a given input. Typically, large incident optical power is required to obtain the optical bistability. However, it can be reduced significantly by using a PhC resonator by enhancing the light-matter interactions.

The nonlinear effects leading to bistable behaviors can be either electronic or thermal. The speeds of electric and thermal nonlinearities are associated with carrier lifetime and thermal relaxation time, respectively. While the thermal effects can be easily induced, its application to information processing is limited because of the slow speed in the megahertz range. However, the electronic nonlinearity allows faster processing that is limited by carrier lifetime. Recently, Tanabe *et al.* have reported fast bistable operation using a silicon PhC resonator with threshold power of 0.4 mW .⁶ Here the electrons are injected via two-photon absorption.

In this report, we demonstrate the optical bistability and all-optical switching based on the electronic nonlinearity using a five-cell two-dimensional PhC linear nanocavity by employing the fiber-coupling technique.⁷ Highly nonlinear InGaAsP four quantum wells (QWs) are employed to reduce unwanted thermal effects.

The hexagonal periodic-hole lattice is chosen and fabricated by electron beam lithography followed by Ar/Cl₂ chemically assisted ion beam etching,⁸ as shown in Fig. 1(a). The lattice constant and hole radius are 460 nm and 160 nm , respectively. The InGaAsP slab contains four QWs of In_{0.76}Ga_{0.24}As_{0.75}P_{0.25} emitting photons near at 1550 nm . Previously, we reported a cavity design having coupling effi-

ciency over 80% by introducing small holes into the linear resonator.⁹ However, since the major fraction of the resonant energy locates in the region of small air holes, this structure is not suitable for applications that require large nonlinearities. For this reason, we design a PhC resonator with Q factor of 25 000 by filling in five air holes. Figure 1(b) shows the photon density distribution calculated by contour finite-difference time-domain (FDTD) simulation using the digitized image of the fabricated structure. The Q factor calculated by the contour image of the fabricated structure is 4170. This reduction of the Q factor is ascribed to the imperfection of our fabrication. The effective mode volume¹⁰ is $0.66a^3$, where a is the lattice constant.

The conventional single-mode fiber is tapered down and strongly bent. The diameter and the radius of curvature are ~ 1.5 and $\sim 50 \mu\text{m}$, respectively [Fig. 2(b)]. Figure 2(a) shows the schematic of our experimental setup. Here, the tunable ($1510\text{--}1640 \text{ nm}$) laser diode is used as an input. By locating the curved microfiber on the surface of the five-cell linear PhC cavity,¹¹ photons stored in the PhC resonator are evanescently coupled with the microfiber. In this configuration, the total Q factor decreases to ~ 2500 , due mainly to the coupling losses into the newly generated TM modes.⁹

Experimentally, transmission characteristics are firstly measured by scanning the wavelength from 1608 to 1614 nm using the continuous wave (cw) sources for various input powers into the fiber, as shown in Fig. 3(a). The cavity resonance is located at the wavelength of 1610.84 nm and the Q factor of the PhC resonator with the fiber is measured to be 2200. The coupling efficiency⁹ with the taper fiber is $\sim 20\%$. The cavity resonance blueshifts with input power. It means that the refractive index change (Δn) is negative and the nonlinearity is dominantly of electronic nature. The refractive index change is measured to be -0.0021 at the input power of $60 \mu\text{W}$. This index change is attributed to the high photon density inside the PhC resonator. As shown in Fig. 4(a), the refractive index change (Δn) shows linear dependency in the region of input powers less than $75 \mu\text{W}$. However, at higher powers, the linear dependency breaks down because of the positive thermal nonlinearity and the higher-order effects.

In Fig. 3(a), we observe discontinuous drops at certain wavelengths for input power higher than $37 \mu\text{W}$. In order to

^{a)}Electronic mail: kmk1852@kaist.ac.kr

^{b)}Also at Department of Physics, Chonnam National University, Gwangju 500-757, Korea.

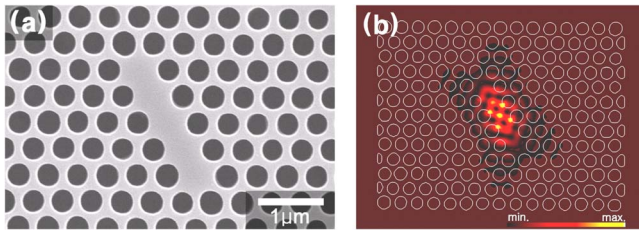


FIG. 1. (Color online) (a) Fabricated five-cell linear PhC slab and (b) photon density distribution by contour FDTD for our fabricated structure shown in Fig. 1(a).

understand these phenomena, the coupled-mode analyses are employed^{12,13} and a simple nonlinear relation ($n=n_0+n_2I$) is assumed. The single resonant mode coupled with a fiber is described as

$$\frac{d\varphi(t)}{dt} = i\omega_0\varphi(t) + i\omega_0\left(\frac{|\varphi|^2}{\varphi_0^2}\right)\varphi(t) - \frac{1}{2}\left(\frac{1}{\tau_{\text{cavity}}} + \frac{1}{\tau_{\text{fiber}}} + \frac{1}{\tau_{\text{abs}}}\right)\varphi(t) + \sqrt{\frac{1}{2\tau_{\text{fiber}}}}s(t). \quad (1)$$

Here, $|\varphi|^2$ and $|s|^2$ are the energies in the resonator and the incidence power, respectively. τ_{cavity} and τ_{fiber} represent the resonator photon lifetime and the coupling time with the fundamental waveguide mode and $1/\tau_{\text{abs}}$ is the absorption loss. Optical nonlinearities are included in the second term in the right side of Eq. (1) with a constant φ_0 .¹⁴ The next two terms indicate the total loss of the resonator and the pumping through the microfiber, respectively. To obtain Fig. 3(b), we use the nonlinear refractive index (n_2) of $-6.84 \times 10^{-14} \text{ m}^2/\text{W}$ that is estimated from Fig. 4(a).¹² The energy confinement factor ($\eta=0.83$) and the effective mode volume ($V_{\text{eff}}=0.66a^3$) are calculated by the FDTD computation.

In the simulation of Fig. 3(b), transmission has a single output for all wavelengths when input power is less than $37 \mu\text{W}$. However, at higher powers, two output values are observed during up- and downward sweeps of input wavelength. When we increase the wavelength from 1608 to 1614 nm, the output shows a discontinuous drop at a certain wavelength for power larger than $37 \mu\text{W}$, as shown in Fig. 3(a). With increasing input power, the spectral position of the downward switching shifts to the shorter wavelength. These characteristics agree well with our measurements in Fig 3(a).

In order to confirm bistable behaviors directly, we inject cw light around 1610 nm. The input beam is polarized to excite TE-like modes in the resonator. Hysteretic behaviors appear when the transmitted power is plotted against the input power [Fig. 4(b)]. Clearly, two output states are observed

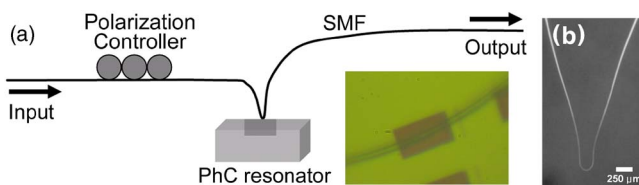


FIG. 2. (Color online) (a) Experimental schematic and (b) curved microfiber used in experiment.

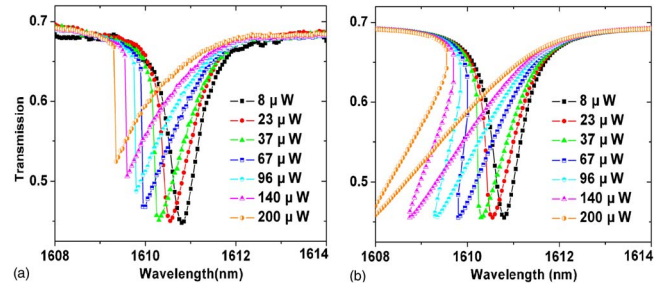


FIG. 3. (Color online) (a) Measured transmission spectra and (b) calculated transmission spectra.

for input powers between 35 and $40 \mu\text{W}$ for a detuning of $\delta=-1.724$. Here δ is the normalized detuning defined as $\delta \equiv (\lambda_{\text{inj}} - \lambda_{\text{res}}) / (\Delta\lambda_{\text{res}}/2)$, where λ_{inj} and λ_{res} are the wavelengths of the input source and the cavity resonance. $\Delta\lambda_{\text{res}}$ indicates the full width at half maximum in the transmission spectrum that is measured to be 0.732 nm. The hysteretic behavior does not appear when the detuning is smaller than -1.724 . This value agrees well with the theoretical threshold detuning, $\delta_0 = -\sqrt{3} \approx -1.732$, that comes from Eq. (1). Hence, the threshold bistable power is close to $35 \mu\text{W}$ and this value compares well with the minimum power of $37 \mu\text{W}$ that shows a sudden drop in the transmission spectrum. The size of the bistable loop increases with detuning. We would like to emphasize that no instability is observed under cw operation for input power $< 200 \mu\text{W}$. Generally, the instability implies a competition between the negative electronic and positive thermal nonlinearities. Our results imply the dominance of the band-edge nonlinearity over the thermal effect. However, when the input power is higher than $200 \mu\text{W}$, the instability does appear.

All-optical switching operation is also demonstrated by using switching pulses at 980 nm, far from the band gap, as shown in Fig. 5(a). Here, the bandwidths of the pulse generator and the photo detector are 100 and 125 MHz, respectively. The probe signal wavelength is fixed at 1610.2 nm. The probe power is set at $37 \mu\text{W}$. As shown in Fig. 5(b), the probe signal (solid line) stays in the upper state in the beginning. When the switching pulse (dotted line) is injected, the probe signal switches to the lower state. Here, the apparent time delay between the switching pulse and downward transition is ascribed to our slow electronic circuit. The minimum switching energy is 75.4 fJ that equals the peak switching power ($5.8 \mu\text{W}$) multiplied by the pulse width (13.0 ns).

In summary, we demonstrate optical bistabilities and all-optical switching in five-cell linear PhC slab cavities under continuous-wave pumping conditions, by employing the fiber-coupling technique. The threshold bistable power is

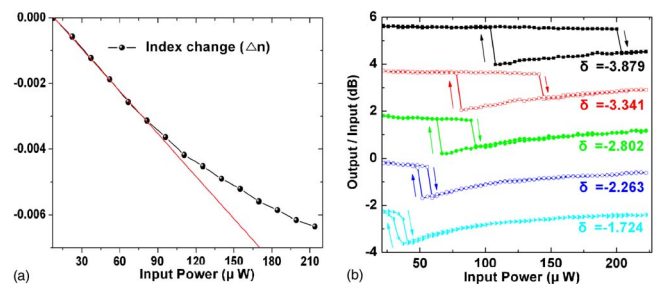


FIG. 4. (Color online) (a) Measured refractive index change (Δn) and (b) bistable curves in decibel scale for various detunings.

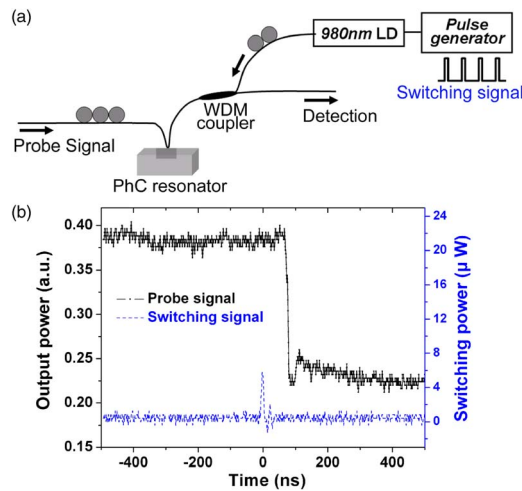


FIG. 5. (Color online) (a) Experimental schematic of all-optical switching and (b) optical switching action.

measured to be $35 \mu\text{W}$ at the normalized detuning of -1.724 for the PhC resonator with a Q factor of 2200. The low-power optical bistability originates from the band-edge resonant nonlinear effect of QWs. The measured bistable actions are in good agreement with theoretical results with the nonlinear refractive index (n_2) of $-6.84 \times 10^{-14} \text{ m}^2/\text{W}$. Particularly, the minimal instability is observed owing to the high band-edge nonlinearities of quantum wells and the efficient fiber coupling. In addition, all-optical switching is demonstrated with pulse energy less than 75.4 fJ . We believe that these low-power bistable devices based on PhC resonators

will be an important building block for the photonic integrated circuits

This work was supported by the National Research Laboratory Project of Korea and the Korea Science and Engineering Foundation (KOSEF) grant funded by the Korea government (MOST).

- ¹T. Yoshie, A. Scherer, J. Hendrickson, G. Khitrova, H. Gibbs, G. Rupper, C. Ell, O. Shchekin, and D. Deppe, *Nature (London)* **432**, 200 (2004).
- ²P. E. Barclay, K. Srinivasan, and O. Painter, *Opt. Express* **13**, 801 (2005).
- ³H. G. Park, S. H. Kim, S. H. Kwon, Y. G. Ju, J. K. Yang, J. H. Baek, S. B. Kim, and Y. H. Lee, *Science* **305**, 1444 (2004).
- ⁴Y. Akahane, T. Asano, B. Song, and S. Noda, *Appl. Phys. Lett.* **83**, 1512 (2003).
- ⁵H. M. Gibbs, *Optical Bistability: Controlling Light with Light* (Academic, New York, 1985), Chap. 1, pp. 4–17.
- ⁶T. Tanabe, M. Notomi, S. Mitsugi, A. Shinya, and E. Kuramochi, *Opt. Lett.* **30**, 2575 (2005).
- ⁷K. Srinivasan, P. E. Barclay, M. Borselli, and O. Painter, *Phys. Rev. B* **70**, 081306(R) (2004).
- ⁸H. Y. Ryu, H. G. Park, and Y. H. Lee, *IEEE J. Sel. Top. Quantum Electron.* **8**, 891 (2002).
- ⁹I. K. Hwang, G. H. Kim, and Y. H. Lee, *IEEE J. Quantum Electron.* **42**, 131 (2006).
- ¹⁰O. Painter, R. K. Lee, A. Scherer, A. Yariv, J. D. O'Brien, P. D. Dapkus, and I. Kim, *Science* **284**, 1819 (1999).
- ¹¹I. K. Hwang, S. K. Kim, J. K. Yang, S. H. Kim, S. Lee, and Y. H. Lee, *Appl. Phys. Lett.* **87**, 131107 (2005).
- ¹²H. A. Haus, *Waves and Fields in Optoelectronics* (Prince-Hall, Englewood cliffs, NJ, 1984), Chap. 10, pp. 288–294.
- ¹³M. F. Yanik, S. Fan, and M. Soljacic, *Appl. Phys. Lett.* **83**, 2739 (2003).
- ¹⁴ φ_0 is determined by the refractive index (n_2), the energy confinement factor (η), and the effective mode volume (V_{eff}), which is described as $\varphi_0^2 = V_{\text{eff}} (\eta/n_2 c)^{-1}$ in Ref. 12.